Journal for ImmunoTherapy of Cancer

Alum-anchored IL-12 combined with cytotoxic chemotherapy and immune checkpoint blockade enhanced antitumor immune responses in head and neck cancer models

Kellsye P Fabian ,[1] Ginette Santiago-Sanchez,[1] Michelle R Padget,[1] Wiem Lassoued,[1] Clint Tanner Allen ,[2] Sailaja Battula,[3] Howard Kaufman,[3] James W Hodge [1]

To cite: Fabian KP, Santiago-Sanchez G, Padget MR, *et al*. Alum-anchored IL-12 combined with cytotoxic chemotherapy and immune checkpoint blockade enhanced antitumor immune responses in head and neck cancer models. *Journal for ImmunoTherapy of Cancer* 2024;**12**:e009712. doi:10.1136/jitc-2024-009712

► Additional supplemental material is published online only. To view, please visit the journal online (https://doi.org/10.1136/jitc-2024-009712).

Accepted 07 October 2024

Check for updates

© Author(s) (or their employer(s)) 2024. Re-use permitted under CC BY-NC. No commercial re-use. See rights and permissions. Published by BMJ.

[1]Center for Immuno-Oncology, Center for Cancer Research, National Cancer Institute, National Institutes of Health, Bethesda, Maryland, USA
[2]Surgical Oncology Program, Center for Cancer Research, National Cancer Institute, National Institutes of Health, Bethesda, Maryland, USA
[3]Ankyra Therapeutics, Cambridge, Massachusetts, USA

Correspondence to
Dr James W Hodge;
jh241d@nih.gov

ABSTRACT

Background First-line treatment with pembrolizumab plus chemotherapy in recurrent and metastatic head and neck squamous cell carcinomas (HNSCC) has improved survival. However, the overall response rate with this standard of care regimen (SOC) remains limited. Interleukin (IL)-12 is a potent cytokine that facilitates the crosstalk between innate and adaptive immunity, making it crucial in the antitumor response. Alum-anchored murine IL-12 (mANK-101) has been demonstrated to elicit robust antitumor responses in diverse syngeneic models, which were correlated with increased immune effector functions and prolonged local retention of IL-12. This study investigates the therapeutic benefit of combining mANK-101 with SOC in the MOC1 and MOC2 murine HNSCC tumor models.

Methods MOC1 and MOC2 tumor-bearing C57BL/6 mice were administered with a single intratumoral injection of mANK-101 and weekly intraperitoneal injections of cisplatin and α-programmed death 1 (PD-1) for 3 weeks. For MOC1, flow cytometry and cytokine array were performed to assess the immune effector functions associated with the combinational treatment. Multiplex immunofluorescence was employed to characterize the influence of the treatment on the immune architecture in the tumors. RNA analysis was implemented for in-depth examination of the macrophage and effector populations.

Results In the MOC1 and MOC2 models, combination therapy with mANK-101, cisplatin, and α-PD-1 resulted in superior tumor growth inhibition and resulted in the highest rate of tumor-free survival when compared with treatment cohorts that received mANK-101 monotherapy or SOC treatment with α-PD-1 plus cisplatin. Furthermore, the combination therapy protected against tumor re-growth on rechallenge and controlled the growth of distal tumors. The improved therapeutic effect was associated with increased $CD8^+$ T-cell recruitment, increased $CD8^+$ and $CD4^+$ activity, and repolarization of the macrophage population from M2 to M1 at the tumor site. Elevated and prolonged interferon-γ expression is central to the antitumor activity mediated by the combination therapy. In addition, the combination therapy with mANK-101+cisplatin+α-PD-1 induced the formation of tertiary lymphoid structure-like immune aggregates in the peritumoral space.

Conclusion The current findings provide a rationale for the combination of alum-tethered IL-12 with cisplatin and α-PD-1 for HNSCC.

WHAT IS ALREADY KNOWN ON THIS TOPIC

⇒ Standard-of-care treatment with pembrolizumab plus chemotherapy results in increased overall survival; however, response rates remain limited.
⇒ Alum-tethered interleukin (IL)-12 (mANK-101) results in high retention of the cytokine in the tumor, thereby promoting robust antitumor immunity in diverse murine tumor models without the toxicities associated with systemic IL-12.

INTRODUCTION

Head and neck cancers rank as the sixth most common malignancy worldwide, with 890,000 new cases per year currently, with a projected increase of up to 1.08 million new cases annually by 2030.[1–3] 90% of all head and neck cancers originate from the mucosal epithelium of the oral cavity, pharynx, and larynx, and are known collectively as head and neck squamous cell carcinomas (HNSCC).[2] Risk factors associated with HNSCC are previous infections with oncogenic strains of human papillomavirus (HPV), tobacco-derived carcinogens, alcohol consumption, and betel nut use.[1 2] The current standard of care (SOC) for recurrent or metastatic (R/M) HNSCC is the programmed death 1 (PD-1) inhibitor pembrolizumab, as monotherapy or in combination with platinum-based chemotherapy plus 5-fluorouracil (5-FU).[4–6] Although durable benefits have

J Immunother Cancer: first published as 10.1136/jitc-2024-009712 on 23 October 2024. Downloaded from http://jitc.bmj.com/ on October 24, 2024 at NIH Library Consortia. Protected by copyright.

WHAT THIS STUDY ADDS

⇒ This study demonstrates that in a murine head and neck tumor model, the combination of alum-tethered IL-12 with cisplatin and α-programmed death 1 (PD-1) confers improved therapeutic benefit compared with mANK-101 alone or standard treatment with cisplatin and α-PD-1.

⇒ In addition to promoting effector immune cell recruitment and activity, the combination therapy skewed the macrophage population from M2 to M1 phenotype and induced the formation of tertiary lymphoid structure-like immune aggregates.

⇒ This is the first report to demonstrate that anchored IL-12 can enhance the efficacy of regimens that combine cytotoxic chemotherapy and checkpoint inhibition.

⇒ The study provides additional insight into the mechanisms of action of anchored IL-12 alone and in combination with chemoimmunotherapy on injected and un-injected tumors.

HOW THIS STUDY MIGHT AFFECT RESEARCH, PRACTICE OR POLICY

⇒ This study identifies alum-anchored IL-12 as a potential combination partner or next-line therapy for first-line treatment with α-PD-1 plus chemotherapy in head and neck squamous cell carcinomas (HNSCC). A clinical study of this combination in relapsed HNSCC, aimed at improving the proportion of patients that respond, is warranted.

been achieved with this combination, only about one-third of patients demonstrate objective responses and it is therefore imperative to improve the SOC regimen to treat HNSCC.

Interleukin-12 (IL-12), a pleiotropic proinflammatory cytokine produced by antigen-presenting cells (APCs), can orchestrate complex crosstalk between the adaptive and innate immunity, inducing the cytotoxic effect of $CD8^+$ T cells, natural killer (NK) cells and natural killer T (NKT) cells, as well as triggering the Th1 differentiation.[7] But despite its potency, the development of IL-12-based therapy has been hampered by suboptimal clinical efficacy and toxicity caused by systemic IL-12 accumulation.[8] Therefore, strategies to enhance and prolong IL-12 responses while minimizing treatment-related toxicities are paramount. Different strategies to localize IL-12 to the tumor site, including intratumoral (i.t.) injection of IL-12-encoding plasmid or messenger RNA and subcutaneous injection of IL-12-based immunocytokine, have shown efficacy in preclinical tumor models[9] and were well-tolerated in a several phase I trials.[10–14] Due to its frequent superficial location and local recurrence pattern, HNSCC is amenable to the intratumoral administration of novel therapeutic agents,[15] including alum-tethered IL-12.

Recently, the development of a novel alum-tethered IL-12 has opened the possibility of an effective and safe IL-12 delivery system.[16 17] It is composed of recombinant IL-12 fused to an aluminum (alum) binding peptide (ABP) co-expressed with a single kinase (Fam20C) that allows a site-specific phosphorylation of the serine residues on the ABP. The phosphorylated ABP binds tightly to the hydroxyl groups of the US Food and Drug Administration-approved vaccine adjuvant aluminum hydroxide (Alhydrogel) to form a stable complex. When injected i.t., the IL-12-ABP/Alhydrogel complex, designated ANK-101, forms a depot, allowing for longer retention of the IL-12 in the tumor and addressing the limitation of i.t. cytokine administration of rapid drug clearance.[16 17] The murine surrogate of ANK-101, known as mANK-101, has been proven to have antitumor efficacy across several hot (MC38 and CT26) and cold (4T1, and B16F10) syngeneic models.[16 17] Furthermore, previous studies have shown that mANK-101 can synergize with checkpoint inhibitors to improve tumor-free survival. In the preclinical models, mANK-101 treatment resulted in increased effector recruitment, upregulated proinflammatory responses, and remodeling of the tumor microenvironment (TME).[16 17]

This study shows for the first time the antitumor efficacy of mANK-101 in combination with cisplatin and α-PD-1 in the HPV-negative MOC1 and MOC2 head and neck tumor models. Combination therapy elicited a robust antitumor response and prolonged survival benefit when compared with mANK-101 monotherapy or with SOC treatment composed of cisplatin plus α-PD-1. The antitumor response mediated by the combination therapy was strongly associated with increased $CD8^+$ T-cell tumor infiltration and cytotoxicity, $CD4^+$ T-cell activity, NK cell maturation, and repolarization of macrophage population from M2 to M1 at the tumor site. Furthermore, interferon (IFN)-γ was found to be a key player in the antitumor response induced by the combination. In addition, combination therapy with mANK-101+cisplatin+α-PD-1 induced the formation of tertiary lymphoid structure (TLS)-like immune aggregates in the MOC1 tumor model. Overall, the current findings provide preclinical rationale for the addition of mANK-101 to the first line SOC for loco-regionally relapsed HNSCC to determine if the proportion of the patients who objectively respond and benefit can be increased.

MATERIALS AND METHODS

Cell lines, animals, and reagents

Original stocks of MOC1 and MOC2 cells were obtained from R. Uppaluri at Washington University (St. Louis, Missouri, USA) and were cultured as described.[18] Cell lines were used at low (<20) passage number and were verified to be free of *Mycoplasma*. Wild-type C57BL/6 mice were bred, housed, and maintained at the National Institutes of Health (Bethesda, Maryland, USA) under pathogen-free conditions in microisolator cages.

Murine IL-12-ABP (mIL-12-ABP), which has been previously described,[16] was provided through a Cooperative Research and Development Agreement between Ankyra Therapeutics (Cambridge, Massachusetts, USA) and the National Cancer Institute (Bethesda, Maryland, USA). The mANK-101 complex was prepared by mixing 0.25 mg/mL mIL-12-ABP with 2.5 mg/mL Alhydrogel (InvivoGen, San Diego, California, USA) in Tris-buffered

J Immunother Cancer: first published as 10.1136/jitc-2024-009712 on 23 October 2024. Downloaded from http://jitc.bmj.com/ on October 24, 2024 at NIH Library Consortia. Protected by copyright.

saline (TBS) buffer for 30 min at room temperature. The complex was used within 4 hours of preparation.

In vivo experiments

All animal studies were approved and conducted in accordance with the NIH Institutional Animal Care and Use Committee approved animal protocol CIO-2 and using ARRIVE1 reporting guidelines.[19] On day 0, female C57BL/6 mice aged 8–12 weeks old were implanted subcutaneously (s.c.) on the right flank with 5×10^6 MOC1 or with 1×10^5 MOC2 cells mixed at 1:1 ratio with Matrigel. For dual-flank studies, cells were inoculated s.c. on the same day on the right and left flanks. For most of the experiments, mANK-101 (5 µg in 20 µL volume) was injected i.t. on day 10, when the mean tumor volume reached 120–200 mm^3. 5 mg/kg cisplatin (West-Ward Pharmaceuticals, Eatontown, New Jersey, USA) and 200 µg α-PD-1 (Clone RMP1-14; Bio X Cell, Lebanon, New Hampshire, USA) were injected intraperitoneally (i.p.) on days 10, 17, and 24. For the depletion studies, 100 µg α-CD4 (Clone GK1.5), 100 µg α-CD8 (2.43), and 100 µg α-NK1.1 (PK136) antibodies were administered i.p. on days 6, 7, and 8, and then once weekly thereafter. 100 µg α-IFN-γ (XMG1.2) and 300 µg α-CSFR1 (AFS98) antibodies were administered i.p. on days −2, 0, and +2 days before and after each treatment, then 3×/week thereafter. All depleting antibodies were acquired from Bio X Cell (Lebanon, New Hampshire, USA). Tumor volume was calculated as length×$width^2$/2. Mice were euthanized when tumor length reached 20 mm, tumor volume exceeded 2,000 mm^3, tumor ulceration covered 50% of the surface, or weight loss exceeded 20%.

Flow cytometry

Excised tumors were mechanically and enzymatically dissociated to generate single-cell suspensions. Cells were exposed to CD16/32 FcR blocking antibodies (Clone 2.4G2; BD Biosciences, Franklin Lakes, New Jersey, USA) prior to staining with primary conjugated antibodies. The following murine antibodies from BioLegend (San Diego, California, USA) were used: CD44-BV421 (clone IM7), CD4-BV605 (RM4-5), IFNγ-BV785 (XMG1.2), granzyme B-FITC (GB-11), CD38-BV421 (90), F4/80-BV605 (BM8), and CD206-PECy7 (C06802). The following antibodies from BD Biosciences (Franklin Lakes, New Jersey, USA) were used: CD62L-BV711 (MEL-14), CD8-PerCP-Cy5.5 (53–6.7), CD3-APC-Cy7 (17A2), CD11b-PerCP-Cy5.5 (M1/70), CD49b-PE (DX5), CD27- PECy7 (LG3A10), CD11c-FITC (HL3), and CD19-APC (ID3). The following antibodies from Invitrogen (Waltham, Massachusetts, USA) were used: CD45-BUV737 (30-F11), FoxP3-PE (FJK-16s), and Ki67-PECy7 (SolA15). Tetramer staining was performed using H-2Kb MuLV p15E Tetramer-KSPWFTTL-APC paired with CD8-PE (Clone KT15) both from MBL International Corporation (Woburn, Massachusetts, USA). Intracellular staining was performed using the FoxP3/transcription factor kit (eBioscience, San Diego, California, USA) per the manufacturer's recommendations. Dead cells were excluded via live/dead fixable blue stain set (Thermo Fisher, Waltham, Massachusetts, USA). All analyses were performed on a BD Fortessa (BD Biosciences, Franklin Lakes, New Jersey, USA) analyzer running FACSDiva software and interpreted using FlowJo V.10.8.2 (TreeStar, Ashland, Oregon, USA). Cell populations were gated on FSC×SSC followed by FSC-A× FSC-H discrimination. Immune cell populations were identified as follows: CD4+T cells: live/CD45+/CD3+/CD4+/CD8−/FoxP3−; CD8+T cells: live/CD45+/CD3+/CD4−/CD8+; regulatory T cells (Tregs): live/CD45+/CD3+/CD4+/CD8−/FoxP3+; NK: live/CD45/CD3−/CD49b+; macrophages: live/CD45+/CD3−/CD11c−/CD19−/CD11b+/F4/80+.

Multiplex cytokine array

Cytokine analysis was performed on sera and tumors using the LEGENDplex Mouse Inflammation Panel (BioLegend, San Diego, California, USA) according to the manufacturer's instructions. Sera were processed from blood samples collected via mandibular bleed. Tumor supernatants were generated via homogenization of tumors in phosphate-buffered saline using the gentleMACS Dissociator (Miltenyi Biotec, Bergisch Galdbach, Germany).

H&E staining, multiplex immunofluorescence staining, and multispectral imaging

Tumors were excised, formalin-fixed, and sent to VitroVivo Biotech (Gaithersburg, Maryland, USA) for paraffin-embedding, sectioning, and H&E staining. For immunofluorescence-staining, the Tyramine Signal Amplification Opal 6-Plex Kits were used according to the manufacturer's protocol (Akoya Biosciences, Marlborough, Massachusetts, USA). The multiplex immunofluorescence panel included DAPI, CD11c, CD103, CXCL13, B220, CD19, and CD8. Deparaffinizing, rehydration, epitope retrieval and staining of slides were performed using the BOND RX Autostainer (Leica, Nussloch, Germany). The optimum staining condition for each antibody was determined using standard immunohistochemistry and single immunofluorescence staining before the combination. Details on antibodies, protocol and opals used in this panel are described in online supplemental table 1. H&E and multiplex immunofluorescence whole slide scans were captured using the scanner PenoImager HT (Akoya Biosciences, Marlborough, Massachusetts, USA) at 20× magnification.

Immune aggregate quantification

Immune aggregates per whole sections were manually quantified based on the multiplex immunostaining. These were classified as tightly associated $B220^+CD19^+$ B cells, $CD8^+$ T cells, and $CD11c^+$ dendritic cells (DC) with CXCL13 and CD103 expression. Areas where cells or markers were present but dispersed were not considered as immune aggregates. Aggregation of cells were confirmed by the respective H&E staining.

J Immunother Cancer: first published as 10.1136/jitc-2024-009712 on 23 October 2024. Downloaded from http://jitc.bmj.com/ on October 24, 2024 at NIH Library Consortia. Protected by copyright.

RNA analysis

Excised tumors were mechanically and enzymatically dissociated to generate single-cell suspensions. For each treatment group, equal numbers of live cells were pooled from each tumor. Immune cell isolation was performed on the pooled cells using the Mouse CD45 Isolation Kit (Miltenyi Biotec, Bergisch Galdbach, Germany) per the manufacturer's instructions. Total RNA was extracted from the isolated cells using the RNeasy Mini Kit (Qiagen, Hilden, Germany) and was analyzed using the nCounter PanCancer Immune Profiling Panel and the nCounter Mouse Myeloid Innate Immunity Gene Expression Panel (NanoString Technologies, Seattle, Washington, USA) by the Genomics Laboratory, Frederick National Laboratory for Cancer Research. Gene expression analyses were done using the nSolver analysis software V.4.0.70 (NanoString Technologies, Seattle, Washington, USA) with housekeeping genes as the normalizing controls and the untreated samples as the categorical reference value followed by core analysis using the Ingenuity Pathway Analysis (Qiagen) with −1.5 and 1.5 as the expression fold change cut-off. The abundance of various cell populations was calculated on ROSALIND using the NanoString Cell Type Profiling Module.

Statistical analysis

One-way or two-way analysis of variance was used to compare more than two groups with Tukey's post hoc analysis for correction. Log-rank (Mantel-Cox) test was used to compare survival curves. Fisher's exact test was applied for pathway analyses. P values <0.05 were considered significant. Error bars represent mean±SEM. GraphPad Prism V.10.2.3 was used to analyze data and generate graphs.

RESULTS

Combination therapy with mANK-101, cisplatin, and α-PD-1 elicits antitumor effect in the MOC1 and MOC2 murine oral squamous cell carcinoma models

The α-PD-1 antibody pembrolizumab with platinum-based chemotherapy (cisplatin or carboplatin) plus fluorouracil is currently the recommended first-line treatment for R/M HNSCC.[4 6] To test the efficacy of this SOC regimen in a murine HNSCC model, MOC1 tumor-bearing mice were treated with weekly injections of α-PD-1 in combination with 5-FU and cisplatin. Since a study on locally advanced HNSCC demonstrated that patients treated with concomitant carboplatin+5 FU completed chemotherapy less frequently than patients treated with cisplatin due to toxicity,[20] the efficacy of α-PD-1 and cisplatin without 5-FU was also tested. Both cisplatin+α-PD-1 (p=0.0105) and 5-FU+cisplatin+α-PD-1 (p=0.0426) had significant but modest antitumor effect in the MOC1 tumor model (online supplemental figure S1A) and no overt adverse effects (online supplemental figure S1B). Based on these data, cisplatin+α-PD-1 was henceforth used as SOC in this study.

mANK-101 is composed of a single chain murine IL-12 containing the p40 and p35 sequences fused to a C-terminal phosphorylated ABP complexed with Alhydrogel.[16 17] Previous studies have shown that i.t. mANK-101 injection resulted in antitumor activity in different syngeneic tumor models associated with the local retention of the IL-12 complex. Here, it was confirmed that mANK-101 inhibited tumor growth of MC38 of different genotypes, with the monotherapy efficacy diminishing with increasing tumor volume at the time of injection (online supplemental figure S2).

To determine whether the addition of mANK-101 can potentiate the antitumor activity of SOC in the MOC1 tumor model, a single i.t. injection of mANK-101 was administered in combination with weekly systemic treatments of cisplatin and α-PD-1 (figure 1A). Cisplatin+α-PD-1 treatment slowed tumor growth (p<0.0001; figure 1B) and improved survival (p=0.0013; figure 1D) when compared with control but did not result in any tumor-free animals (figure 1C). Meanwhile, mANK-101 monotherapy resulted in improved tumor growth control compared with untreated (p<0.0001) and SOC (p=0.003; figure 1B), with 2 out of 10 animals being tumor-free at the end of the study (figure 1C) and in prolonged survival compared with untreated (p<0.0001) and SOC (p=0.0094; figure 1D). But ultimately, mANK-101+cisplatin+α-PD-1 resulted in a superior tumor growth inhibition compared with untreated (p<0.0001), mANK-101 (p=0.0194), and SOC (p<0.0001; figure 1B). The mANK-101+cisplatin+α-PD-1 combination treatment also resulted in the greatest number of tumor-free animals at 5 out of 10 (figure 1C) and improved median overall survival compared with untreated (p=0.0001), mANK-101 (p=0.0153), and cisplatin+α-PD-1 (p=0.0002; figure 1D). Furthermore, in an alternative treatment schedule wherein mANK-101 injection was given 1 week after starting the cisplatin+α-PD-1 injections, the triple combination still successfully outperformed mANK-101 (p=0.009) and SOC (p=0.0138; online supplemental figure S3) treatments. Compared with mANK-101+5 FU+cisplatin+α-PD-1, mANK-101+cisplatin+α-PD-1 resulted in a similar antitumor response and safety profile (online supplemental figures S1C and S1D), further supporting the sufficiency of using cisplatin+α-PD-1 as SOC for the MOC1 model. mANK-101+cisplatin+α-PD-1 also protected the mice from tumor recurrence with 66.6% of the tumor-free mice inhibiting tumor regrowth when challenged with 5×10^6 MOC1 cells (figure 1E). Previous therapy with mANK-101+cisplatin+α-PD-1 also improved the survival of the re-challenged animals compared with naïve mice implanted with the tumor (p=0.0005; figure 1F).

Cytokine analysis revealed that the antitumor effect observed with the mANK-101+cisplatin+α-PD-1 combination was associated with increased tumoral IL-12 and IFN-γ levels (figure 1G,H). Tumoral IL-12 was augmented in the mANK-101+cisplatin+α-PD-1 treated group on day 15 (p=0.0134) and remained persistently high on day 22 (figure 1G; p=0.0248). In contrast, serum IL-12

J Immunother Cancer: first published as 10.1136/jitc-2024-009712 on 23 October 2024. Downloaded from http://jitc.bmj.com/ on October 24, 2024 at NIH Library Consortia. Protected by copyright.

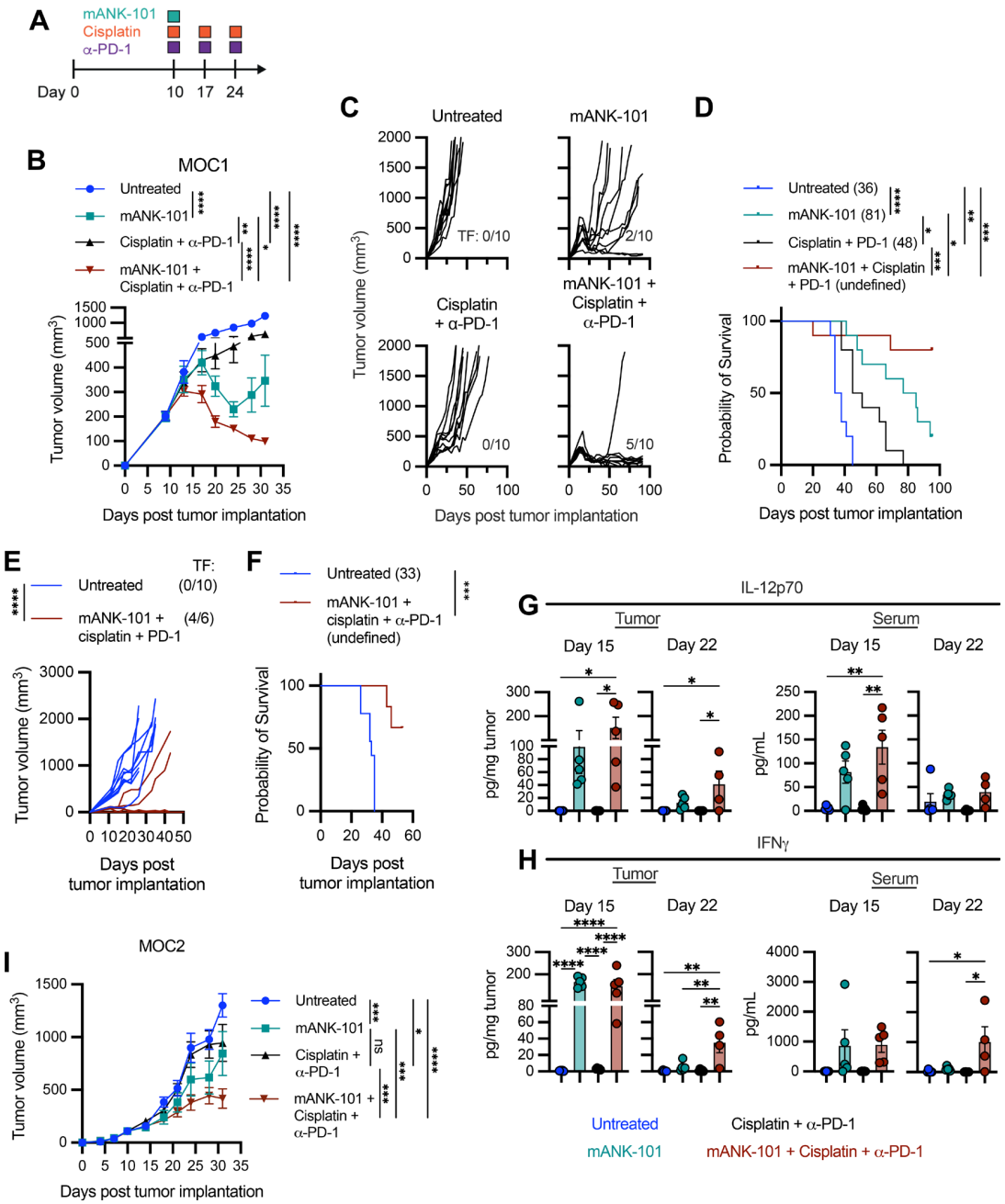

Figure 1 Combination therapy with mANK-101, cisplatin, and α-PD-1 elicits antitumor effect in the MOC1 and MOC2 murine oral squamous cell carcinoma models. (A–D) Female C57BL/6 mice (8–12 weeks old; n=10/group) were implanted with 5×10^6 MOC1 cells on the right flank on day 0 and treated with a single i.t. injection of 5 µg mANK-101 on day 10, when the tumor volume average was ~200 mm^3. The mice were also treated with cisplatin (5 mg/kg, i.p.), and α-PD-1 (200 µg, i.p.) on days 10, 17, and 24 as described in (A) the treatment schematic diagram. Tumor growth was monitored. (B) Mean and (C) individual growth curves are presented. Insets denote the number of animals that were tumor-free at the end of the study. (D) Animal survival was followed, with number in parentheses indicating the mOS. (E–F) A new cohort of MOC1 tumor-bearing animals was treated as described in A. On day 55, tumor-free animals resulting from the triple therapy were re-challenged with 5×10^6 MOC1 cells. Naïve C57BL/6 mice were used as untreated controls. (E) Tumor growth mean and (F) survival post-tumor rechallenge were monitored. (G–H) Female C57BL/6 mice (8–12 weeks old; n=8/group) were implanted on the right and left flanks with 5×10^6 MOC1 cells each. The mice were treated as described in A. Sera and primary tumors (n=4–5/group) were collected on days 15 and 22. The samples were analyzed for (G) IL-12p70 and (H) IFN-γ via multiplex cytokine array. (I) Female C57BL/6 mice (8–12 weeks old; n=8/group) were implanted with 1×10^5 MOC2 cells and were treated as described in A. Tumor growth was monitored and mean tumor volume is shown. Statistical tests: tumor growth: two-way ANOVA with Tukey's post hoc test; survival: Mantel-Cox test; comparison between groups: one-way ANOVA with Tukey's post hoc test. Error bars, SEM. *p<0.05, **p<0.01, ***p<0.001, ****p<0.0001. ANOVA, analysis of variance; IFN, interferon; i.p., intraperitoneal; mOS, median overall survival; ns, not significant; PD-1, programmed death 1; TF, tumor-free.

J Immunother Cancer: first published as 10.1136/jitc-2024-009712 on 23 October 2024. Downloaded from http://jitc.bmj.com/ on October 24, 2024 at NIH Library Consortia. Protected by copyright.

was elevated on day 15 (p=0.0134) but was back to baseline level on day 22 (figure 1G). mANK-101 monotherapy (p<0.0001) and mANK-101+cisplatin+α-PD-1 treatment (p<0.0001) resulted in high tumoral IFN-γ on day 15 compared with control (figure 1H). However, by day 22, tumoral IFN-γ was back to baseline levels with mANK monotherapy, while it remained significantly elevated in the mANK-101+cisplatin+α-PD-1 treated group (p=0.0018; figure 1H). Although not statistically significant, mANK-101 monotherapy and mANK-101+cisplatin+α-PD-1 treatments boosted IFN-γ levels by 10-fold in the serum on day 15 (figure 1H). On day 22, only the mANK-101+cisplatin+α-PD-1 treated animals maintained significantly increased levels of IFN-γ in the serum (p=0.0368; figure 1H). Together, the data suggest that mANK-101+cisplatin+α-PD-1 treatment induces a sustained pro-inflammatory signature in the tumor.

Immunogenic tumors, such as MOC1, are more likely to respond to immunotherapy.[21 22] Hence, the efficacy of the mANK-101+cisplatin+α-PD-1 combination therapy was tested in the poorly immunogenic MOC2 tumor.[21] In this model, mANK-101 monotherapy and cisplatin+α-PD-1 treatment only moderately inhibited tumor growth compared with control (p=0.003 and p=0.0263, respectively; figure 1I). Meanwhile, mANK-101+cisplatin+α-PD-1 therapy significantly suppressed tumor growth when compared with untreated (p<0.0001), mANK-101 (p=0.0005), and cisplatin+α-PD-1 (p=0.0001) treatment groups. Overall, the data suggest that the mANK-101+cisplatin+α-PD-1 combination is associated with sustained IL-12 and IFN-γ levels in the tumor and is effective against immunogenic and recalcitrant oral squamous cell carcinoma tumor models.

mANK-101 in combination with α-PD-1 has been shown to significantly enhance antitumor activity in diverse murine tumor models.[16 17] Hence, it was investigated whether combination therapy with mANK-101+α-PD-1 or with mANK-101+cisplatin is sufficient to reduce MOC1 tumor growth. While mANK-101+cisplatin resulted in tumor regression compared with control (p=0.0006), its efficacy was statistically equivalent to that of mANK-101 monotherapy (p=0.8843; figure 2A). Likewise, mANK-101+α-PD-1 treatment was potent against MOC1 tumors (p=0.0004), but its activity was the same as mANK-101 monotherapy (p=0.6797, figure 2B). As demonstrated in figure 1, mANK-101+cisplatin+α-PD-1 therapy significantly improved antitumor effect over mANK-101 alone based on tumor growth inhibition (p=0.0393; figure 2C) and resulted in the greatest number of tumor-free animals (figure 2D). It should be noted that mANK-101+α-PD-1 treatment resulted in 4 out of 11 mice being tumor-free at the end of the study. This indicates that while there was a superior antitumor response with mANK-101+cisplatin+α-PD-1 therapy, there still may be a substantial therapeutic advantage with mANK-101+α-PD-1, especially in terms of achieving a tumor-free endpoint. All the treatments and combinations tested were safe and had no adverse effects on the health of the animals based on lack of severe weight loss (figure 2E).

Combination therapy with mANK-101, cisplatin, and α-PD-1 promotes antitumor immune responses

To explore changes in the immune landscape on treatment, RNA analysis using the NanoString nCounter Mouse PanCancer IO360 Panel Kit was performed on CD45 cells isolated from tumors 5 days after the first round of treatments. Gene expression analysis shows that mANK-101 monotherapy and mANK-101+cisplatin+α-PD-1 combination treatment resulted in the increased expression of cytokines, chemokines, and factors associated with the innate and adaptive immune responses, with Ifng as the most upregulated gene for both groups (figure 3A). Consequently, pathway analysis shows that immune cell activation, including T-cell receptor, IL-12, and IFN signaling, as well as antigen presentation, were promoted in the mANK-101 monotherapy and mANK-101+cisplatin+α-PD-1 combination cohorts (figure 3B). Cell type profiling showed that cytotoxic T cells were enriched in the mANK-101+cisplatin+α-PD-1 combination group, while exhausted T cells and Tregs were diminished in the mANK-101 monotherapy and mANK-101+cisplatin+α-PD-1 groups (figure 3C).

Flow cytometry was also performed to assess the immune tumor infiltrates. No changes in the frequency of effector $CD4^+$ T cells were observed with any of the treatments (figure 3D) despite the mANK-101+cisplatin+α-PD-1 treatment increasing the fraction of $Ki67^+$ $CD4^+$ T cells (p=0.0054; figure 3E). Frequencies of effector memory (Tem; $CD44^+CD62L^-$) and central memory (Tcm; $CD44^+CD62L^+$) $CD4^+$ T-cell populations also remained similar among the groups (figure 3F). However, compared with the untreated and SOC-treated groups, the functional capabilities, namely IFN-γ and granzyme B expression, of the tumor-infiltrating $CD4^+$ T cells were markedly improved in animals treated with mANK-101 monotherapy and mANK-101+cisplatin+α-PD-1 combination (p<0.0001; figure 3G).

On the other hand, only the mANK-101+cisplatin+α-PD-1 treatment significantly enriched the tumor-infiltrating $CD8^+$ T-cell population (p=0.0021; figure 3H), including $CD8^+Ki67^+$ (p=0.0016; figure 3I), $CD8^+$ Tem and $CD8^+$ Tcm phenotypes (p=0.0020; figure 3J). Examination of the $CD44^+CD8^+$ compartment showed that, compared with control, mANK-101 monotherapy and mANK-101+cisplatin+α-PD-1 combination therapy augmented the IFN-γ expression (p=0.0462 and p=0.0005, respectively) and IFN-γ+granzyme B double expression (p=0.347 and p=0.007, respectively; figure 3K). MOC1 tumor cells expressed the endogenous retroviral envelope protein p15e[21] and, notably, mANK-101+cisplatin+α-PD-1 combination therapy significantly expanded the p15e-tetramer$^+$ $CD8^+$ T cells in the TME (figure 3L), indicating the ability of this treatment modality to elicit an antigen-specific response against the tumor.

The suppressive Treg cell population in the TME was decreased with mANK-101 (p<0.0001) and mANK-101+cisplatin+α-PD-1 (p<0.0001) treatments (figure 3M). Although this reduction in Tregs did not result in

J Immunother Cancer: first published as 10.1136/jitc-2024-009712 on 23 October 2024. Downloaded from http://jitc.bmj.com/ on October 24, 2024 at NIH Library Consortia. Protected by copyright.

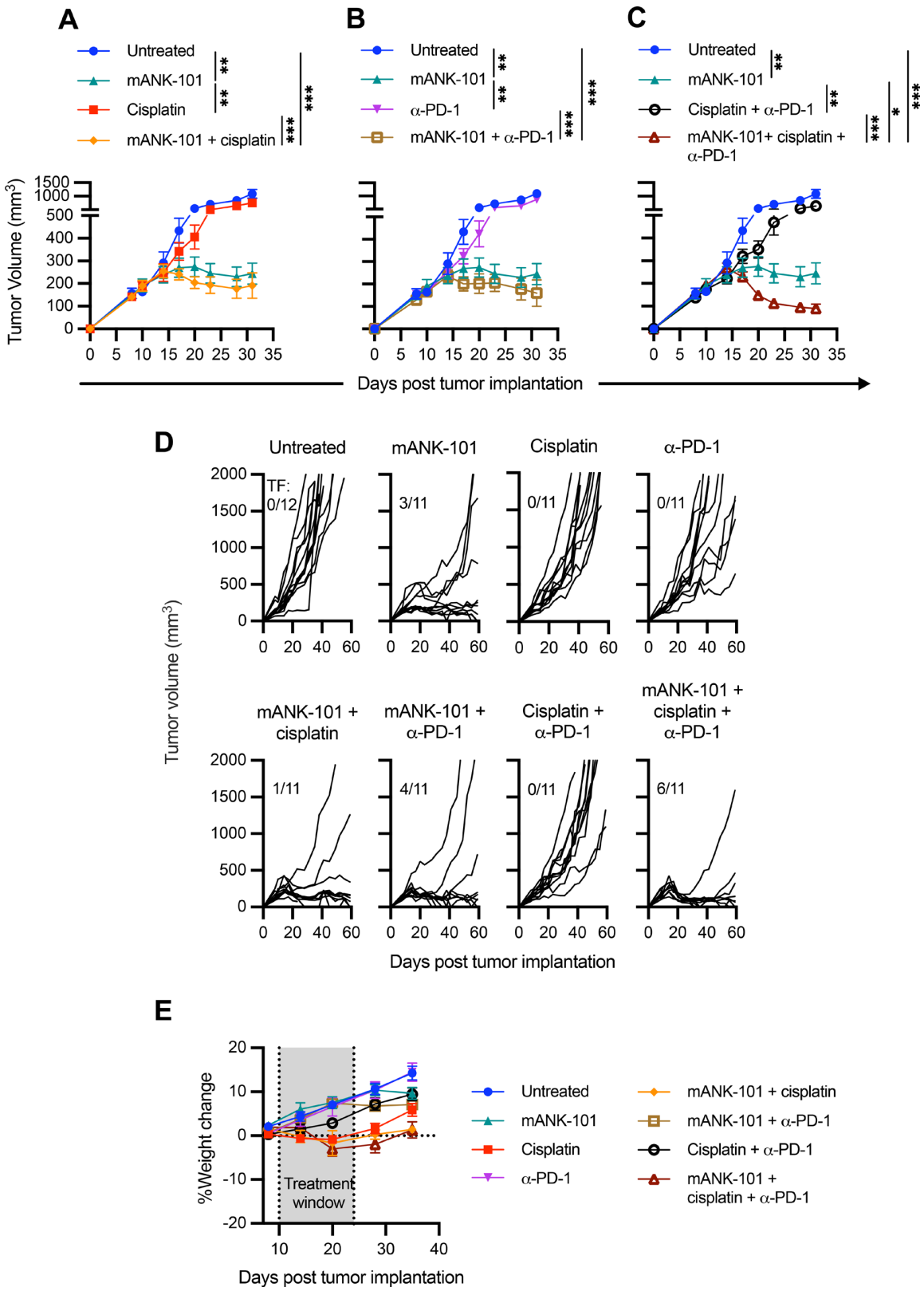

Figure 2 Combination therapy with mANK-101, cisplatin, and α-PD-1 elicits a superior antitumor effect compared with monotherapy and double combination therapy. Female C57BL/6 mice (8–12 weeks old; n=11–12/group) were implanted with 5×10^6 MOC1 cells on the right flank on day 0, were treated as described in figure 1A, and were monitored. (A–C) Mean and (D) individual growth curves are presented. Insets denote the number of animals that were tumor-free at the end of the study. (E) Body weight changes over time were also monitored. Statistical tests: tumor growth: two-way ANOVA with Tukey's post hoc test. Error bars, SEM. *p<0.05, **p<0.01, ***p<0.001. ANOVA, analysis of variance; PD-1, programmed death 1; TF, tumor-free.

J Immunother Cancer: first published as 10.1136/jitc-2024-009712 on 23 October 2024. Downloaded from http://jitc.bmj.com/ on October 24, 2024 at NIH Library Consortia. Protected by copyright.

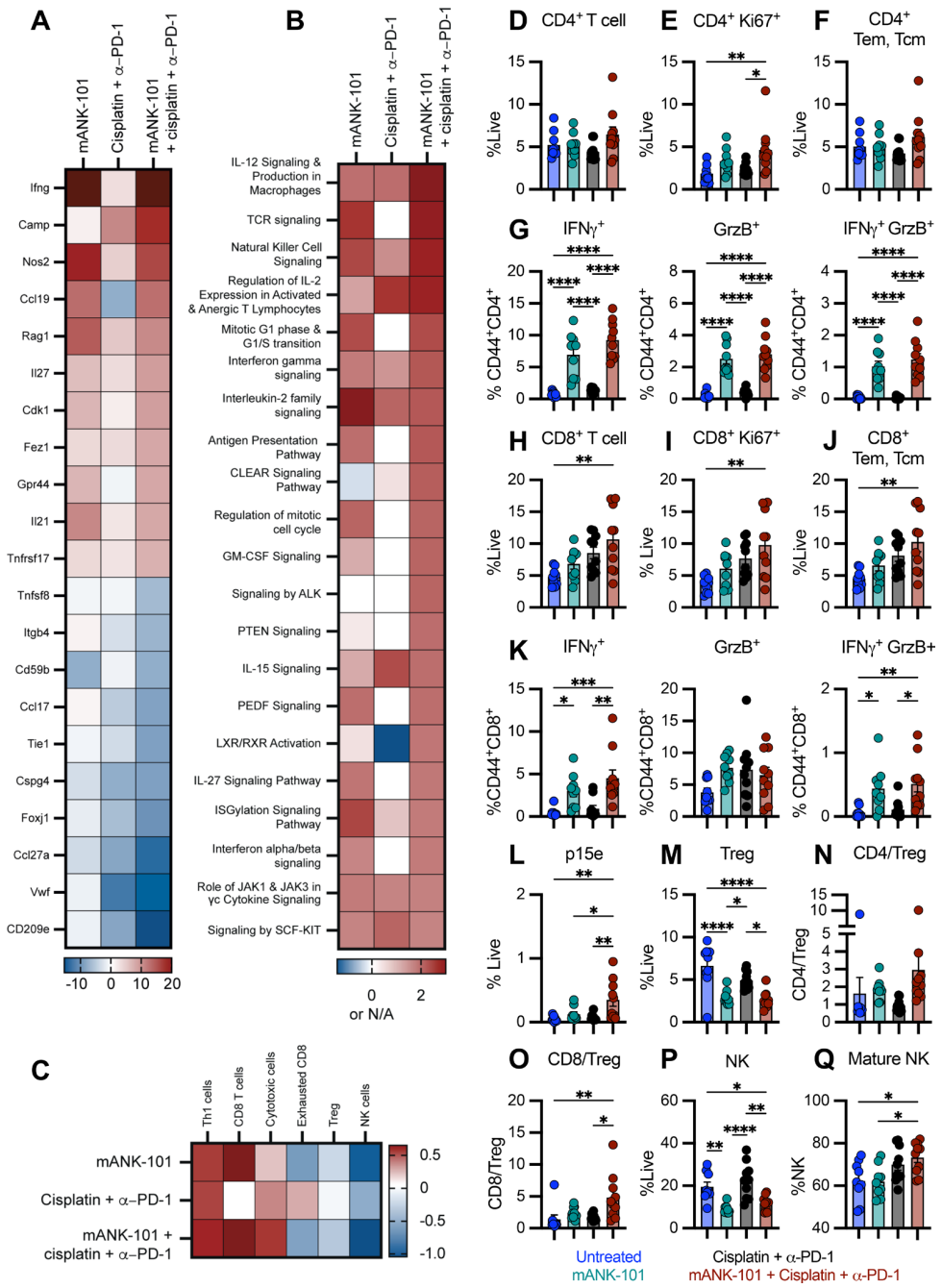

Figure 3 Combination therapy with mANK-101, cisplatin, and α-PD-1 promotes antitumor immune responses. (A–C) Female C57BL/6 mice (8–12 weeks old; n=5–10/group) were implanted with 5×10^6 MOC1 cells on the right flank on day 0 and were treated with mANK-101 (5 µg, i.t.), cisplatin (5 mg/kg, i.p.), and α-PD-1 (200 µg, i.p.) on day 10. On day 15, gene expression analysis was performed on tumor-infiltrating CD45$^+$ cells by NanoString Mouse PanCancer IO360. Heatmaps showing (A) the top 10 upregulated and downregulated transcripts in the combination group compared with the untreated control based on fold-change, (B) the pathway enrichment analysis based on z-score and (C) cell type profiles based on cell type z-score. (D–Q) On day 15, flow cytometric analysis was performed to determine (D) the frequency of CD4$^+$ T cells, (E) the frequency of Ki67$^+$ CD4$^+$ T cells and (F) the frequency of memory CD4 T cells. The CD44$^+$CD4$^+$ compartment was further analyzed for the frequency of (G) IFN-γ$^+$, granzyme B$^+$, and IFN-γ$^+$granzyme B$^+$ cells. The frequencies of (H) CD8$^+$ T cells, (I) Ki67$^+$ CD8$^+$ T cells and (J) memory CD8 T cells were also determined. Likewise, the CD44$^+$CD8$^+$ T cells that were interrogated for (K) IFN-γ$^+$, granzyme B$^+$, and IFN-γ$^+$ granzyme B$^+$ expression. Staining was also performed to identify (L) p15e tetramer-positive CD8$^+$ T cells as well as (M) FoxP3$^+$CD4$^+$ Treg cells. (N) CD4/Treg and (O) CD8/Treg ratios were calculated. (P) The frequency of CD49b$^+$ NK cells, as well as (Q) the frequency of NK cells that are mature (CD11b$^+$) were determined. Statistical tests: one-way ANOVA with Tukey's post hoc test. Error bars, SEM *p<0.05, **p<0.01, ***p<0.001, ****p<0.0001. ANOVA, analysis of variance; GrzB, granzyme B; IFN, interferon; i.p., intraperitoneal; i.t., intratumoral; N/A, not applicable; NK, natural killer; PD-1, programmed death 1; Tcm, central memory T cell; Tem, effector memory T cell; Treg, regulatory T cell.

J Immunother Cancer: first published as 10.1136/jitc-2024-009712 on 23 October 2024. Downloaded from http://jitc.bmj.com/ on October 24, 2024 at NIH Library Consortia. Protected by copyright.

improved CD4:Treg ratio in these groups (figure 3N), the concomitant increase in $CD8^+$ T cells on mANK-101+cisplatin+α-PD-1 treatment significantly enhanced the CD8:Treg ratio (p=0.0071; figure 3O).

Unexpectedly, the frequency of NK cells in the TME declined in the mANK-101 and mANK-101+cisplatin+α-PD-1 treatment groups (figure 3P), yet the fraction of mature NK cells, comprising $CD11b^+CD27^+$ and $CD11b^+CD27^-$ NK cells, was enhanced in the mANK-101+cisplatin+α-PD-1 treatment group compared with control (p=0.0286) and mANK-101 group (p=0.0236; figure 3Q).

Combination therapy with mANK-101, cisplatin, and α-PD-1 results in the emergence of immune aggregates in the MOC1 tumor

The immune infiltrates in the tumor were also examined via H&E and multiplex immunofluorescence staining 28 days post tumor implantation. H&E staining detected aggregates of immune cells in the peritumoral region of some of the MOC1 tumors, most of which were from animals treated with mANK-101 monotherapy and mANK-101+cisplatin+α-PD-1 combination therapy (figure 4A, rightmost panels). Immunofluorescent staining revealed that these immune aggregates are composed of $B220^+CD19^+$ B cells cell clusters with $CD11c^+$ DCs interspersed and surrounded by $CD8^+$ T cells, including $CD103^+CD8^+$ tissue-resident memory T cells (figure 4A, middle and rightmost panels). This organization of the immune cells is characteristic of TLSs that have been observed in different human and murine tumor samples.[23 24] It is suspected that the p15e-specific $CD8^+$ T cells detected via flow cytometry (figure 3L) are situated in these immune aggregates and must be confirmed via immunofluorescence staining using tetramer probes on fresh tissue sections in future experiments.[25 26] Furthermore, CXCL13 expression, which has been associated with the formation and maintenance of ectopic lymphoid structures,[27 28] was detected in the immune aggregates in the MOC1 samples. Quantification of the immune aggregates demonstrated the increased presence of TLS-like clusters in the tumor on mANK-101+cisplatin+α-PD-1 combination therapy (figure 4B). Notably, the increased B-cell infiltration and formation of immune aggregates promoted by the mANK-101+cisplatin+α-PD-1 treatment was also associated with elevated circulating anti-MOC1 tumor antibodies in this treatment cohort (online supplemental figure S4). These findings are consistent with reports that suggest that TLS promote response to immunotherapy.[29 30]

The antitumor immune response elicited by mANK-101, cisplatin, and α-PD-1 triple combination therapy is dependent on an IFN-γ response

Next, depletion studies were performed to determine which immune components are essential for the therapeutic effect elicited by mANK-101+cisplatin+α-PD-1 combination therapy. Concurrent, but not individual, depletion of $CD8^+$ T cells, $CD4^+$ T cells, and NK cells diminished the ability of mANK-101+cisplatin+α-PD-1 treatment to suppress tumor growth (p<0.0001; figure 5A) and prolong survival (p<0.0001; figure 5B). Furthermore, IFN-γ depletion reduced the tumor growth control (p<0.0001; figure 5C) and the survival advantage that was induced by the combination therapy (p=0.0001; figure 5D). Taken together, the data suggest that effector lymphocytes and IFN-γ play an important role in the activity of the mANK-101+cisplatin+α-PD-1 therapy. However, the intricate and multifaceted response induced by the combination therapy does not appear to rely on one single immune component since complete abrogation was not achieved in any of the depletions.

Combination therapy with mANK-101+cisplatin+α-PD-1 promotes a shift from M2 to M1 in the TME

The majority of tumor-associated macrophages (TAMs) in the TME are derived from circulating monocytes with monocyte chemoattractant protein-1 (MCP-1) acting as one of the main drivers of recruitment.[31 32] MCP-1 was increased in the sera (p=0.003) and tumors (p=0.0007) of animals that received mANK-101+cisplatin+α-PD-1 treatments (figure 6A). Tumoral MCP-1 was also increased in mANK-101-treated mice (p<0.0001; figure 6A). While the increase in MCP-1 did not affect the total macrophage frequency in the TME (figure 6B), it was associated with the expansion of the pro-inflammatory M1 ($CD38^+CD206^-$) macrophages (figure 6C) and the reduction of pro-tumorigenic M2 ($CD38^-CD206^+$) macrophages (figure 6D) in the mANK-101 monotherapy and in the mANK-101+cisplatin+α-PD-1 treatment groups (p<0.0001 for all comparisons vs control). Consequently, the M1/M2 ratio was significantly improved by the mANK-101 (p=0.0325) and mANK-101+cisplatin+α-PD-1 (p=0.0013; figure 6E) treatments.

In line with these observations, RNA analysis using the nCounter Mouse Myeloid Innate Immunity Gene Expression Panel revealed that genes encoding cytokines and chemokines, such as Ifng, Cxcl9, and Cxcl10, that are associated with M1-mediated responses[33] were upregulated in the mANK-101 monotherapy and combination therapy groups (figure 6F). Hence, in these same groups, pathways involved in macrophage activity (eg, antigen presentation) and regulation (eg, LXR/RXR, ubiquitination/deubiquitination) were also promoted (figure 6G). While the mANK-101+cisplatin+α-PD-1 combination resulted in 100% survival of the treated mice, combination therapy with concurrent depletion of macrophages resulted in decreased survival to 62.5% (figure 6H). Although not statistically significant (p=0.0628), the trend suggests that macrophages may have an important role in the therapeutic response.

Combination therapy with mANK-101+cisplatin+α-PD-1 elicits abscopal responses

Recent studies demonstrated that i.t. injection of mANK-101 led to the regression of distal, uninjected lesions in Ag410A, B16F10, and MC38 models.[16 17] To determine whether the abscopal effect can also be observed in the mANK-101+cisplatin+α-PD-1 combination therapy, mice implanted with MOC1 tumors on both flanks were

J Immunother Cancer: first published as 10.1136/jitc-2024-009712 on 23 October 2024. Downloaded from http://jitc.bmj.com/ on October 24, 2024 at NIH Library Consortia. Protected by copyright.

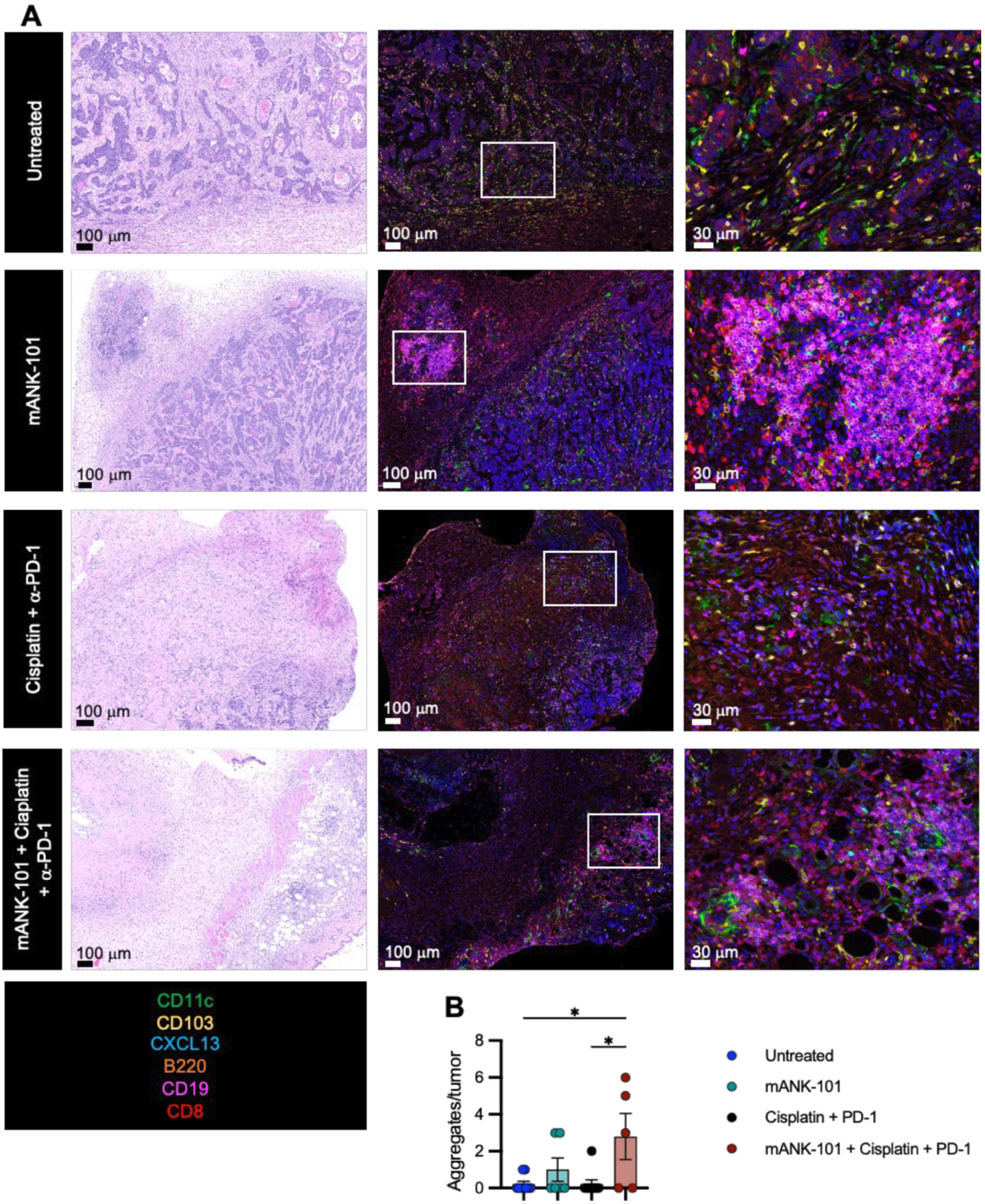

Figure 4 Combination therapy with mANK-101, cisplatin, and α-PD-1 results in the emergence of immune aggregates in the MOC1 tumor. Female C57BL/6 mice (8–12 weeks old; n=8–10/group) were implanted with 5×10^6 MOC1 cells on the right flank on day 0 and were treated as described in figure 1A. On day 28, the tumors were harvested and fixed for (A) H&E (leftmost panels) and multiplex immunofluorescence staining (middle and rightmost panels). (B) Immune aggregates composed of closely associated $B220^+CD19^+$ B cells, $CD11c^+$ DCs, $CD8^+$ T cells with CD103 and CXCL13 expression were counted. Statistical tests: one-way ANOVA with Tukey's post hoc test. Error bars, SEM. *p<0.05. ANOVA, analysis of variance; DC, dendritic cell; PD-1, programmed death 1.

J Immunother Cancer: first published as 10.1136/jitc-2024-009712 on 23 October 2024. Downloaded from http://jitc.bmj.com/ on October 24, 2024 at NIH Library Consortia. Protected by copyright.

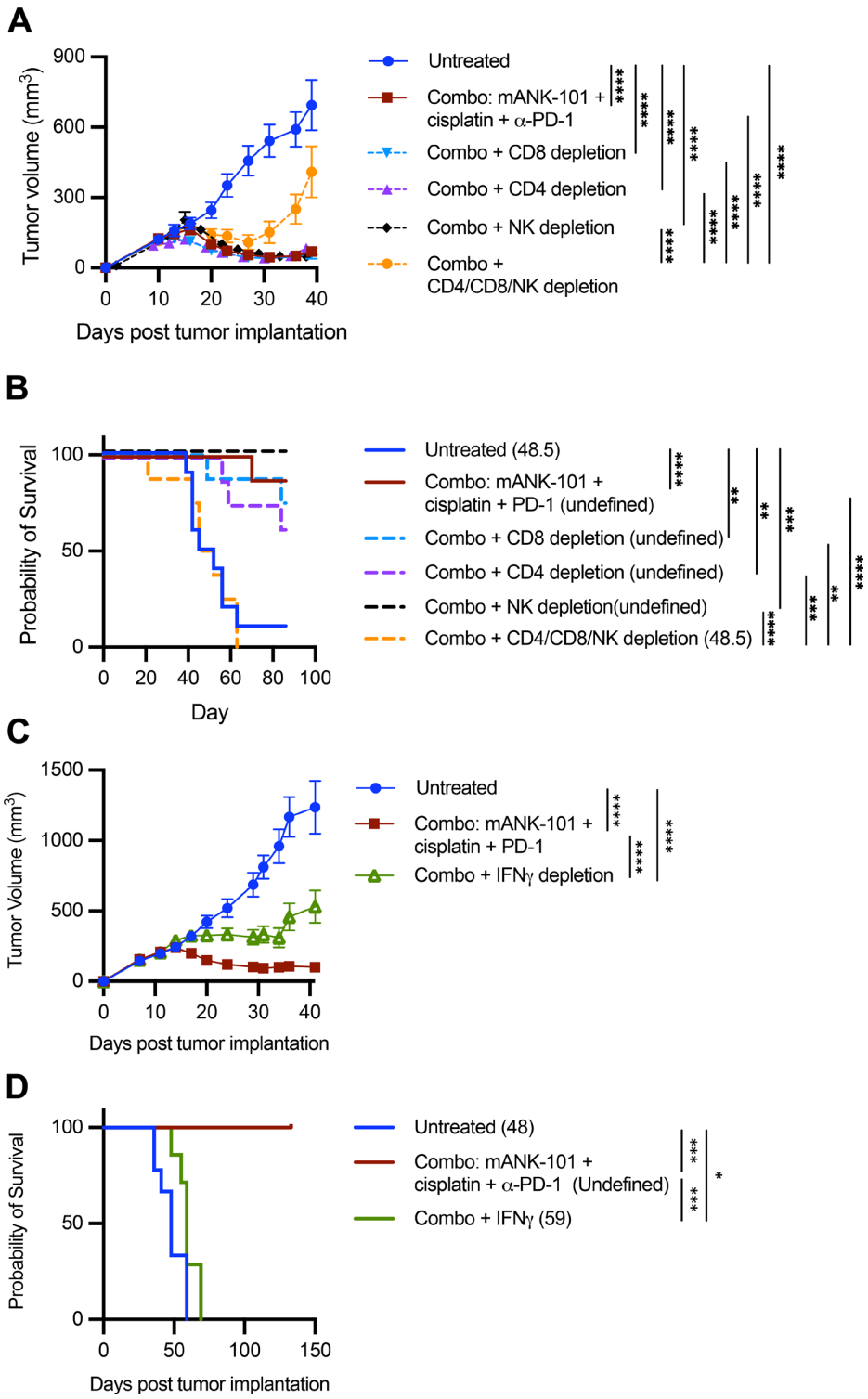

Figure 5 The antitumor immune response elicited by mANK-101, cisplatin, and α-PD-1 triple combination therapy is dependent on an IFN-γ response. Female C57BL/6 mice (8–12 weeks old; n=8–10/group) were implanted with 5×10^6 MOC1 cells on the right flank on day 0 and were treated as described in figure 1A. (A–B) CD4 (100 µg, i.p.), CD8 (100 µg, i.p.), and NK1.1 (100 µg, i.p.) depleting antibodies were administered on days 6, 7, and 8 and then once weekly thereafter. Tumor growth was monitored. (A) Mean tumor volume and (B) survival are shown. Numbers in parentheses indicate mOS. (C–D) IFN-γ blocking antibody (100 µg, i.p) was administered 2 days prior to treatment, same day as treatment, and 2 days after treatment, then 3×/week thereafter. Tumor growth was monitored. (C) Mean tumor volume over time and (D) survival are shown. Statistical tests: tumor growth: two-way ANOVA with Tukey's post hoc test; survival: Mantel-Cox test. Error bars, SEM. *p<0.05, **p<0.01, ***p<0.001, ****p<0.0001. ANOVA, analysis of variance; IFN, interferon; i.p., intraperitoneal; mOS, median overall survival; PD-1, programmed death 1.

J Immunother Cancer: first published as 10.1136/jitc-2024-009712 on 23 October 2024. Downloaded from http://jitc.bmj.com/ on October 24, 2024 at NIH Library Consortia. Protected by copyright.

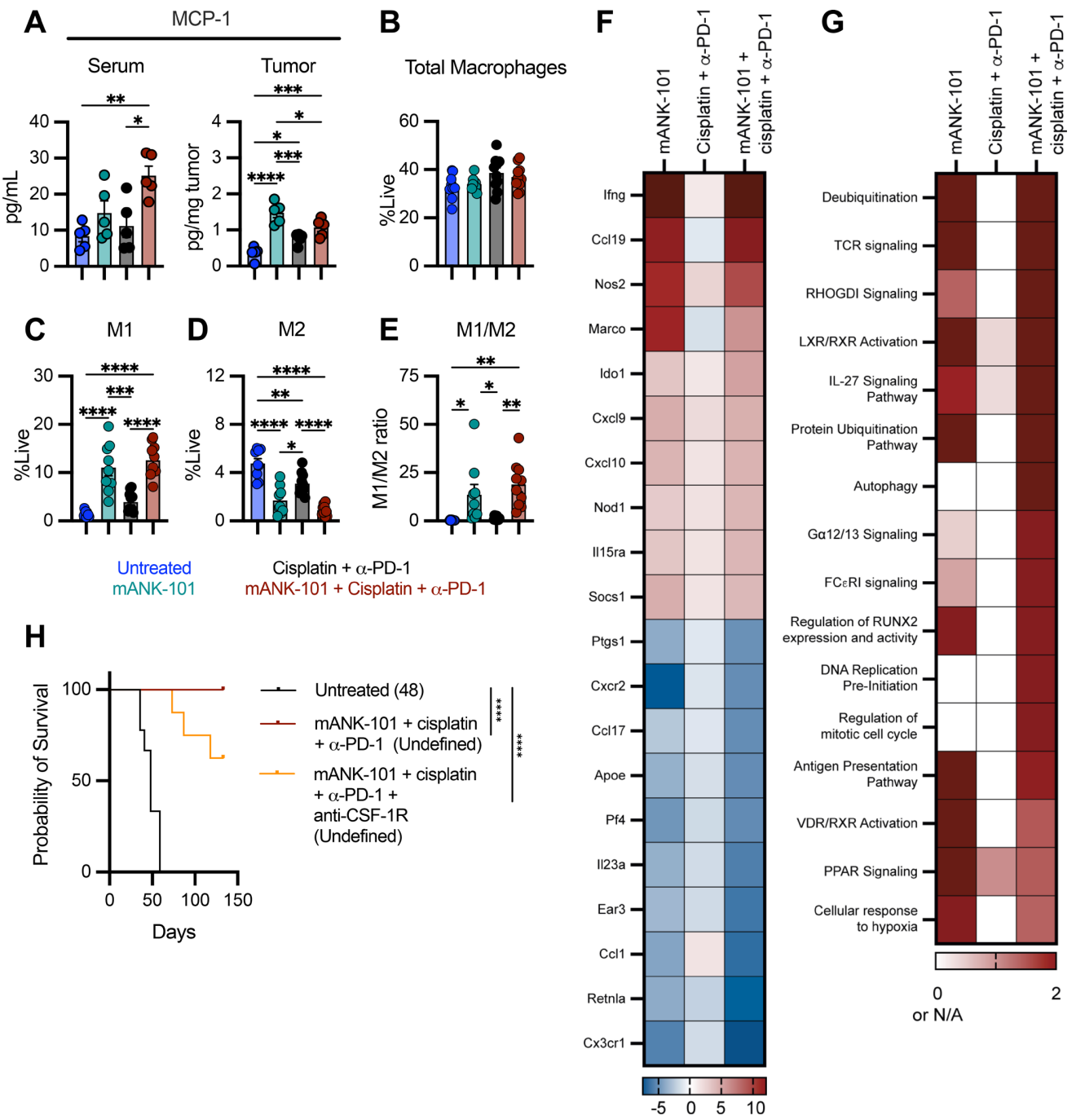

Figure 6 Combination therapy with mANK-101+cisplatin+α-PD-1 promotes a shift from M2 to M1 in the tumor microenvironment. Female C57BL/6 mice (8–12 weeks old; n=8–10/group) were implanted with 5×10^6 MOC1 cells on the right flank on day 0 and were treated with mANK-101 (5 µg, i.t.), cisplatin (5 mg/kg, i.p.), and a-PD-1 (200 µg, i.p.). On day 15, sera and tumors were collected and analyzed for (A) MCP-1 expression. Flow cytometric analysis of the tumor was also performed on day 15 to determine the (B) total macrophage populations ($CD11b^+F4/80^+$) and (C) M1 ($CD11b^+F4/80^+CD38^+CD206^-$) and (D) M2 ($CD11b^+F4/80^+CD38^-CD206^+$) frequencies, from which the (E) M1/M2 ratio was calculated. (F) On day 15, RNA analysis was performed on tumor-infiltrating $CD45^+$ cells by NanoString Mouse Myeloid Innate Immunity Panel. Heatmaps showing (F) the top 10 upregulated and downregulated transcripts in the combination group compared with the untreated control based on fold-change and (G) the pathway enrichment analysis based on z-score are presented. (H) C57BL/6 mice (8–12 weeks old; n=8–10/group) were implanted with 5×10^6 MOC1 cells on the right flank on day 0 and were treated as described in figure 1A. CSFR1 blocking antibody (100 µg, i.p) was administered 2 days prior to treatment, same day as treatment, and 2 days after treatment, then 3 ×/week thereafter. Animal survival was followed. Statistical tests: one-way ANOVA with Tukey's post hoc test; survival: Mantel-Cox test. Error bars, SEM. *p<0.05. ANOVA, analysis of variance; i.p., intraperitoneal; i.t., intratumoral; MCP, monocyte chemoattractant protein; M1, type 1 macrophage; M2, type 2 macrophage; N/A, not applicable; PD-1, programmed death 1.

J Immunother Cancer: first published as 10.1136/jitc-2024-009712 on 23 October 2024. Downloaded from http://jitc.bmj.com/ on October 24, 2024 at NIH Library Consortia. Protected by copyright.

injected with mANK-101 on the right flank and were given systemic cisplatin and α-PD-1 treatments. In this bilateral tumor model, cisplatin+α-PD-1 treatment inhibited the growth of both tumors (p<0.0001; figure 7A). In the injected tumor, mANK-101 monotherapy and mANK-101+cisplatin+α-PD-1 treatment resulted in greater tumor regression compared with control (p<0.0001 for both) and SOC (p=0.0041 and p=0.0011, respectively), but had similar tumor growth inhibition when compared with each other (p=0.9834). However, in the distal tumor, mANK-101 monotherapy resulted in an antitumor effect that was on par with that of the cisplatin+α-PD-1 treatment (p=0.8324), while mANK-101+cisplatin+α-PD-1 combination resulted in significant regression of the distal tumor compared with mANK-101 monotherapy (p=0.0089) and cisplatin+PD-1 regimen (p=0.0006).

Consistent with the data presented in figure 3, flow cytometric analysis of the tumors showed that mANK-101 monotherapy and mANK-101+cisplatin+α-PD-1 treatment increased $CD8^+$ T-cell infiltration (figure 7B), increased p15e-tetramer$^+$ $CD8^+$ populations (figure 7C), increased M1 macrophages (figure 7D), and limited M2 macrophages (figure 7E) in the mANK-101-injected (right) tumor 5 days after first treatment. However, in the distal tumors (left), mANK-101 monotherapy had no effect on these cell populations. The combination therapy, on the other hand, augmented CD8+T cell infiltration (p=0.0319, figure 7B) and promoted the M1 population (p=0.0085; figure 7D) in the distal tumor, although not to the levels observed in the right injected tumor. Cisplatin+α-PD-1 therapy had no significant effect on the select immune cells on the right tumor and the frequency of each population was comparable in the right and left tumors. To investigate the role of $CD8^+$ T cells in the abscopal response, $CD8^+$ T-cell depletion was performed on the MOC1 dual flank model treated with the combination therapy. In the mANK-101 injected (right) tumors, $CD8^+$ T cells were not necessary for the efficacy of the mANK-101+cisplatin+α-PD-1 combination treatment (figure 7F). In the distal tumors, however, $CD8^+$ T-cell depletion significantly reduced the antitumor effect of the combination therapy (p<0.0001; figure 7F). The data suggest that $CD8^+$ T cells play a critical role in the abscopal response elicited by the combination therapy.

Gene expression pathway analysis shows that combination treatment with mANK-101+cisplatin+α-PD-1 induced immune-related pathways in both the injected and distal tumors (figure 7F). Three innate immune signaling pathways, namely NOD1/2, CGAS/STING, and classical macrophage activation, were promoted by the combination therapy in both tumors. Furthermore, in the injected tumors, pathways that were upregulated by the combination treatment were also upregulated by mANK-101 monotherapy. However, in the distal tumors, differential pathway expression was observed between the mANK-101 monotherapy and combination therapy groups. For instance, while cytokine pathways such as IL-27 and IL-12 signaling were upregulated at varying degrees in both groups, the three innate immune signaling pathways mentioned above that were upregulated in the combination therapy group were downregulated in the distal tumors of the cohort that received mANK-101 only.

DISCUSSION

The landmark KEYNOTE-048 clinical trial demonstrated that pembrolizumab alone or with chemotherapy resulted in enhanced overall survival among patients with metastatic or unresectable recurrent HNSCC.[4 6] Based on this study, pembrolizumab alone is now recommended as first-line treatment for programmed death-ligand 1 (PD-L1) positive HNSCC or with chemotherapy (cisplatin or carboplatin plus fluorouracil) for HNSCC independent of PD-L1 status. But while the median overall survival was extended with pembrolizumab alone or with chemotherapy when compared with cetuximab plus chemotherapy, the SOC treatments did not improve progression-free survival or objective response. Furthermore, subgroup analysis demonstrated that the efficacy of pembrolizumab with or without chemotherapy corresponds to the level of PD-L1 expression. In fact, in patients with a PD-L1 combined positive score (CPS) of less than 1, pembrolizumab and pembrolizumab-chemotherapy did not improve overall survival when compared with cetuximab plus chemotherapy.[34] In murine tumor models, mANK-101 has been shown to increase PD-L1 expression in the tumor,[17] which provides a rationale for combining localized IL-12 to the current SOC.

The current study provides preclinical evidence for the application of ANK-101 with SOC chemotherapy and pembrolizumab as a treatment for R/M HNSCC, especially in patients with PD-L1 CPS<1. As demonstrated in the MOC1 tumor model, mANK-101+cisplatin+α-PD-1 combination therapy resulted in enhanced tumor regression and increased rate of tumor-free survival compared with mANK-101 monotherapy and SOC treatment with cisplatin+α-PD-1. This study also necessitates the clinical study of ANK-101 with pembrolizumab alone since antitumor activity was also observed with the doublet in the MOC1 tumor model. Although the current study was evaluated in an HPV-negative tumor, the clinical development of this combination may be extended to include HPV$^+$ patients since clinical consensus guidelines currently do not include HPV status as a determining factor for SOC immunotherapy recommendations for patients with R/M HNSCC.[35] However, in future clinical trials, it would be vital to determine whether response rates to ANK-101 in combination with SOC differ when patients are stratified by HPV status.

The current study confirmed and extended the previous studies that illustrated that anchored mANK-101 elicited a robust antitumor response in diverse syngeneic tumor models when administered as single-agent therapy or in combination with immune checkpoint inhibitors (ICB).[16 17] The antitumor response was associated with the prolonged retention of IL-12 complex in the tumor,

J Immunother Cancer: first published as 10.1136/jitc-2024-009712 on 23 October 2024. Downloaded from http://jitc.bmj.com/ on October 24, 2024 at NIH Library Consortia. Protected by copyright.

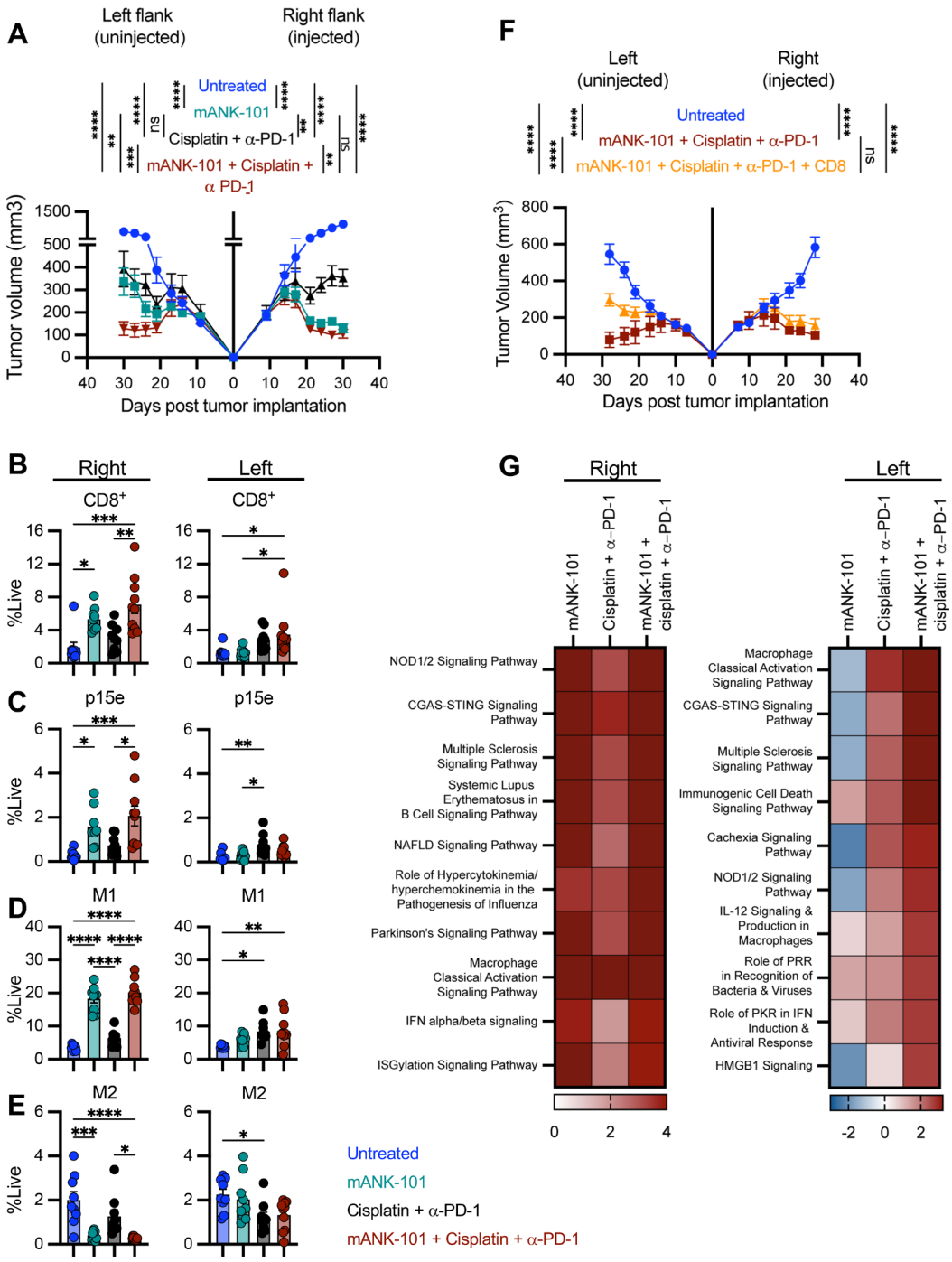

Figure 7 Combination therapy with mANK-101+cisplatin+α-PD-1 elicits abscopal responses. Female C57BL/6 mice (8–12 weeks old; n=8/group) were implanted on the right and left flanks with 5×10^6 MOC1 cells each. The mice were treated as described in figure 1A, with the right flank intratumorally injected with 5 µg mANK-101 and the left flank tumor uninjected. (A) Tumor growth on both flanks was monitored. On day 15, flow cytometric analysis was performed to determine the frequency of (B) $CD8^+$ T cells, (C) p15e tetramer-positive $CD8^+$ T cells, (D) M1 macrophages ($CD11b^+F4/80^+CD38^+CD206^-$) and (E) M2 macrophages ($CD11b^+F4/80^+CD38^-CD206^+$) in the right and left tumors. (F) Female C57BL/6 mice (8–12 weeks old; n=9–10/group) were implanted with 5×10^6 MOC1 cells on the right and left flanks on day 0, were treated as described in figure 1A and were also administered with CD8 (100 µg, i.p.) depleting antibodies on days 6, 7, and 8 and then once weekly thereafter. Tumor growth on both flanks were monitored and presented. RNA analysis was performed on tumor-infiltrating $CD45^+$ cells isolated on day 15 via NanoString Mouse PanCancer IO360 and (G) heatmaps representing enriched pathways in the right and left tumors are shown. Statistical tests: tumor growth: two-way or one-way ANOVA with Tukey's post hoc test; comparison between groups: one-way ANOVA with Tukey's post hoc test. Error bars, SEM. *p<0.05, **p<0.01, ***p<0.001, ****p<0.0001. ANOVA, analysis of variance; IFN, interferon; i.p., intraperitoneal; M1, type 1 macrophage; M2, type 2 macrophage; PD-1, programmed death 1.

J Immunother Cancer: first published as 10.1136/jitc-2024-009712 on 23 October 2024. Downloaded from http://jitc.bmj.com/ on October 24, 2024 at NIH Library Consortia. Protected by copyright.

thereby increasing the therapeutic window while mitigating toxicities. In the current study, IL-12 levels in the tumor were further enhanced at longer durations when mANK-101 was combined with cisplatin and α-PD-1 (figure 1G). Serum IL-12 levels were also transiently elevated before coming down to baseline (figure 1G) but it cannot be determined whether the spike in IL-12 is due to a positive feedback loop that causes even more IL-12 upregulation or leakage. Nevertheless, no toxicities were observed based on the animals maintaining their body weight (figure 2E).

All patients with HNSCC who initially present with metastatic disease and over two-thirds of patients who relapse after definitive treatment have locoregional disease.[36] Like cutaneous malignancies, newly diagnosed or relapsed mucosal head and neck cancers are amenable to local injection.[15] Although safety precautions must be taken due to the risk of local inflammation following mANK-101 injection, the accessibility of newly diagnosed and relapsed mucosal primary tumors to the local injection makes early-phase clinical study of the addition of mANK-101 to SOC feasible.

Previous studies showed that mANK-101 treatment promoted T-cell recruitment and activity in the tumor.[16 17] Preliminary results of the phase I trial of canine ANK-101 (cANK-101) in dogs with advanced oral malignant melanoma also demonstrated that cANK-101 treatments resulted in enhanced immune infiltration into the tumor and elevated circulating IFN-γ.[37] In agreement with these studies, it is observed that the superior antitumor effect of the mANK-101+cisplatin+α-PD-1 combination was associated with increased $CD8^+$ T-cell infiltration and activity (figure 3) and increased tumoral IFN-γ levels (figure 1H). Unexpectedly, $CD8^+$ T-cell depletion did not negatively impact the combination therapy-mediated antitumor response. Reduction in therapeutic benefit with the combination treatment was observed only when $CD4^+$ T, $CD8^+$ T, and NK cells were simultaneously depleted, suggesting that there is a cooperative and/or compensatory interplay among these lymphocyte populations. On the other hand, IFN-γ, which can be produced by different activated immune cells and whose role in tumor regression has been well established,[38] is one of the key players in the antitumor response exerted by mANK-101+cisplatin+α-PD-1 therapy as suggested by the RNA, flow cytometry, and depletion analyses.

In addition, the combination therapy induced a memory response that protected the mice from tumor rechallenge and distal tumors (figures 1E and 7A). Based on the depletion study, $CD8^+$ T cells are required for the abscopal response even though p15e-specific T cells were not detected in the distal tumor (figure 7). The p15e-specific T cells may have had infiltrated at a later time point and/or T cells targeting neoepitopes and other tumor antigens played a bigger role in the distal tumor. Nevertheless, the mANK-101-mediated enhancement of antigen presentation,[16] coupled with augmented T-cell activity stimulated by mANK-101 and PD-1, may have synergized to significantly improve the antitumor efficacy observed with the combination therapy. Moreover, cisplatin can sensitize tumors, rendering them more susceptible to immune attack.[39 40] This may explain why the regression of distal tumors was more pronounced in the combination group versus the mANK-101 monotherapy group.

The TME of HNSCC is densely infiltrated with TAMs, largely composed of the M2 phenotype that facilitates a protumorigenic and immunosuppressive environment and is associated with poor prognosis.[41 42] Hence, the ability of mANK-101+cisplatin+α-PD-1 to repolarize TAMs from M2 to the antitumorigenic M1 phenotype is an important feature that needs to be investigated more thoroughly. MCP-1, a chemokine for monocytic recruitment,[31 32] increased with combination therapy but was not associated with increased total macrophage frequency in the MOC1 tumor (figure 6A,B). There are conflicting reports whether MCP-1 favors M1 or M2 differentiation, although others suggest that the contexture of the tumor, including the cytokine milieu, metabolic health, and other factors, may have more influence on the shift in macrophage phenotype.[32 43] IFN-γ has previously been identified as a main mediator of the polarization and maintenance of M1 macrophages[44 45] and is important in the upregulation of CXCL9 and CXCL10 (figure 6F). Macrophage-derived CXCL9 and CXCL10 are essential in the ICB therapy-mediated response[46] and may contribute to the additive antitumor effect of mANK-101 and SOC in the MOC1 tumor model as well as in other tumor models as reported previously.[17]

The data suggest that one of the key processes of the mANK-101+cisplatin+α-PD-1 therapy-mediated response is the induction of TLS-like immune aggregates. TLSs, characterized by mature DCs juxtaposed within B cell-rich follicles adjacent to T-cell rich zones, have been linked to the establishment of protective antitumor immunity.[23 24 29 30] In these structures, tumor antigens are presented by DCs to T cells, allowing for local immune priming to promote T-cell activation and memory T-cell generation.[23 24] A recent report also demonstrated that major histocompatibility complex-restricted and tumor antigen-specific interactions between B cells and T cells are important in mediating abscopal effects mediated by intratumoral IL-12 plus cytidine monophosphate guanosine oligodeoxynucleotide (CpG) treatment.[47] Although the biology and function of TLSs in cancer are yet to be fully elucidated, the formation of organized immune aggregates in the tumor is thought to contribute to faster and more efficient immune responses and provide a lymphoid niche that can support the function and longevity of effector cells.[24] TLSs have been correlated to increased patient survival in several cancer settings[48–50] and to improved response to immune checkpoint blockade.[29 30] In HNSCC, TLS signatures were found to be more prevalent in patients with HPV^+ HNSCC than in the HPV^- cohort.[51 52] In this study, mANK-101 monotherapy induced the formation of TLS-like immune

J Immunother Cancer: first published as 10.1136/jitc-2024-009712 on 23 October 2024. Downloaded from http://jitc.bmj.com/ on October 24, 2024 at NIH Library Consortia. Protected by copyright.

aggregates in the HPV⁻ MOC1 tumor, which was further enhanced when mANK-101 was administered with cisplatin and α-PD-1 (figure 4). Further interrogation is required to determine whether these aggregates are bona fide TLSs, including the confirmation of the presence of germinal center B cells and follicular DCs as well as the detection of high endothelial venules.[52–54] Nevertheless, these data are consistent with a previous report that showed that intratumoral injection of recombinant IL-12 in patients with HNSCC was associated with extensive B-cell infiltration in the peritumoral space.[55] The mechanism by which mANK-101, cisplatin, and α-PD-1 cooperatively promote TLS-like aggregate formation and whether it differs between HPV⁺ and HPV⁻ human and murine HNSCC must be investigated. In addition, the role of humoral immunity in the antitumor response elicited by the mANK-101+cisplatin+α-PD-1 combination must be further examined. Intratumoral injection of IL-12 Fc and CpG has been associated with the presence of antitumor antibodies in the serum of treated mice.[47] In the current study, the infiltration of B cells (figure 4) and the upregulation of the systemic lupus erythematosus in B-cell signaling pathway[56] (figure 7G) is associated with the production of anti-MOC1 antibodies in the triple combination therapy group. The antigen specificity and the contribution to the antitumor response of these antibodies warrant further investigation.

The ANCHOR study, which is a first-in-human study evaluating the safety, tolerability, pharmacokinetic and pharmacodynamic effects of the human version of mANK-101, is currently underway and will inform future combinations with alum-tethered IL-12. In this current preclinical study, mANK-101+cisplatin+α-PD-1 therapy resulted in improved antitumor response associated with increased effector cell infiltration and activity, formation of TLS-like immune aggregates and improved M1/M2 ratio. Overall, the data presented provide a rationale for combining alum-tethered IL-12 with the standard treatment for HNSCC and suggest that this combination may also be efficacious in patients who have low PD-L1 expression.

Acknowledgements The authors thank Debra Weingarten for her editorial assistance in the preparation of this manuscript.

Contributors KPF, SB, HK, and JWH conceptualized and designed research studies. KPF, GS-S, MRP, WL, CTA, and JWH conducted the experiments and acquired data. KPF, GS-S, WL, and JWH analyzed the data. KPF, GS-S, and JWH wrote the manuscript. KPF, GS-S, MRP, WL, CTA, SB, HK, and JWH reviewed the manuscript. JWH is the guarantor.

Funding This work was funded by the Intramural Research Program of the Center for Cancer Research, National Cancer Institute, National Institutes of Health (ZIA BC 010944), as well as via a Cooperative Research and Development Agreement between the National Cancer Institute and Ankyra Therapeutics (Cambridge, Massachusetts, USA).

Competing interests HK and SB work for Ankyra Therapeutics.

Patient consent for publication Not applicable.

Ethics approval All animal experimental studies were performed under the approval of the NIH Intramural Animal Care and Use Committee. All mice were housed and maintained in accordance with the Association for Assessment and Accreditation of Laboratory Animal Care (AAALAC) guidelines: NIH AALAC approval: CIO-2.

Provenance and peer review Not commissioned; externally peer reviewed.

Data availability statement Data are available upon reasonable request. Not applicable.

Supplemental material This content has been supplied by the author(s). It has not been vetted by BMJ Publishing Group Limited (BMJ) and may not have been peer-reviewed. Any opinions or recommendations discussed are solely those of the author(s) and are not endorsed by BMJ. BMJ disclaims all liability and responsibility arising from any reliance placed on the content. Where the content includes any translated material, BMJ does not warrant the accuracy and reliability of the translations (including but not limited to local regulations, clinical guidelines, terminology, drug names and drug dosages), and is not responsible for any error and/or omissions arising from translation and adaptation or otherwise.

Open access This is an open access article distributed in accordance with the Creative Commons Attribution Non Commercial (CC BY-NC 4.0) license, which permits others to distribute, remix, adapt, build upon this work non-commercially, and license their derivative works on different terms, provided the original work is properly cited, appropriate credit is given, any changes made indicated, and the use is non-commercial. See http://creativecommons.org/licenses/by-nc/4.0/.

ORCID iDs
Kellsye P Fabian http://orcid.org/0000-0002-0273-5647
Clint Tanner Allen http://orcid.org/0000-0001-6586-5804
James W Hodge http://orcid.org/0000-0001-5282-3154

REFERENCES

1 Barsouk A, Aluru JS, Rawla P, *et al*. Epidemiology, Risk Factors, and Prevention of Head and Neck Squamous Cell Carcinoma. *Med Sci (Basel)* 2023;11.
2 Johnson DE, Burtness B, Leemans CR, *et al*. Head and neck squamous cell carcinoma. *Nat Rev Dis Primers* 2020;6:92.
3 Solomon B, Young RJ, Rischin D. Head and neck squamous cell carcinoma: Genomics and emerging biomarkers for immunomodulatory cancer treatments. *Semin Cancer Biol* 2018;52:228–40.
4 Burtness B, Harrington KJ, Greil R, *et al*. Pembrolizumab alone or with chemotherapy versus cetuximab with chemotherapy for recurrent or metastatic squamous cell carcinoma of the head and neck (KEYNOTE-048): a randomised, open-label, phase 3 study. *Lancet* 2019;394:1915–28.
5 Yu C, Li Q, Zhang Y, *et al*. Current status and perspective of tumor immunotherapy for head and neck squamous cell carcinoma. *Front Cell Dev Biol* 2022;10:941750.
6 Harrington KJ, Burtness B, Greil R, *et al*. Pembrolizumab With or Without Chemotherapy in Recurrent or Metastatic Head and Neck Squamous Cell Carcinoma: Updated Results of the Phase III KEYNOTE-048 Study. *J Clin Oncol* 2023;41:790–802.
7 Lasek W, Zagożdżon R, Jakobisiak M. Interleukin 12: still a promising candidate for tumor immunotherapy? *Cancer Immunol Immunother* 2014;63:419–35.
8 Jia Z, Ragoonanan D, Mahadeo KM, *et al*. IL12 immune therapy clinical trial review: Novel strategies for avoiding CRS-associated cytokines. *Front Immunol* 2022;13:952231.
9 Cirella A, Luri-Rey C, Di Trani CA, *et al*. Novel strategies exploiting interleukin-12 in cancer immunotherapy. *Pharmacol Ther* 2022;239:108189.
10 Thaker PH, Brady WE, Lankes HA, *et al*. A phase I trial of intraperitoneal GEN-1, an IL-12 plasmid formulated with PEG-PEI-cholesterol lipopolymer, administered with pegylated liposomal doxorubicin in patients with recurrent or persistent epithelial ovarian, fallopian tube or primary peritoneal cancers: An NRG Oncology/Gynecologic Oncology Group study. *Gynecol Oncol* 2017;147:283–90.
11 Strauss J, Heery CR, Kim JW, *et al*. First-in-Human Phase I Trial of a Tumor-Targeted Cytokine (NHS-IL12) in Subjects with Metastatic Solid Tumors. *Clin Cancer Res* 2019;25:99–109.
12 Gatti-Mays ME, Tschernia NP, Strauss J, *et al*. A Phase I Single-Arm Study of Biweekly NHS-IL12 in Patients With Metastatic Solid Tumors. *Oncologist* 2023;28:364–e217.
13 Castañón E, Zamarin D, Carneiro BA, *et al*. Abstract CT004: Intratumoral (IT) MEDI1191 + durvalumab (D): Update on the first-in-human study in advanced solid tumors. *Cancer Res* 2023;83:CT004.

J Immunother Cancer: first published as 10.1136/jitc-2024-009712 on 23 October 2024. Downloaded from http://jitc.bmj.com/ on October 24, 2024 at NIH Library Consortia. Protected by copyright.

14 Bechter O, Loquai C, Champiat S, *et al*. Abstract LB198: A first-in-human, open-label, multicenter study of intratumoral SAR441000 (mixture of cytokine encoding mRNAs), as monotherapy and in combination with cemiplimab in patients with advanced solid tumors. *Cancer Res* 2023;83:LB198.
15 Jiménez-Labaig P, Rullan A, Braña I, *et al*. Intratumoral therapies in head and neck squamous cell carcinoma: A systematic review and future perspectives. *Cancer Treat Rev* 2024;127:102746.
16 Agarwal Y, Milling LE, Chang JYH, *et al*. Intratumourally injected alum-tethered cytokines elicit potent and safer local and systemic anticancer immunity. *Nat Biomed Eng* 2022;6:129–43.
17 Battula S, Papastoitsis G, Kaufman HL, *et al*. Intratumoral aluminum hydroxide-anchored IL-12 drives potent antitumor activity by remodeling the tumor microenvironment. *JCI Insight* 2023;8:e168224.
18 Judd NP, Allen CT, Winkler AE, *et al*. Comparative analysis of tumor-infiltrating lymphocytes in a syngeneic mouse model of oral cancer. *Otolaryngol Head Neck Surg* 2012;147:493–500.
19 Kilkenny C, Browne WJ, Cuthill IC, *et al*. Improving bioscience research reporting: the ARRIVE guidelines for reporting animal research. *PLoS Biol* 2010;8:e1000412.
20 Hanemaaijer SH, Kok IC, Fehrmann RSN, *et al*. Comparison of Carboplatin With 5-Fluorouracil vs. Cisplatin as Concomitant Chemoradiotherapy for Locally Advanced Head and Neck Squamous Cell Carcinoma. *Front Oncol* 2020;10:761.
21 Moore EC, Cash HA, Caruso AM, *et al*. Enhanced Tumor Control with Combination mTOR and PD-L1 Inhibition in Syngeneic Oral Cavity Cancers. *Cancer Immunol Res* 2016;4:611–20.
22 Duan Q, Zhang H, Zheng J. Turning Cold into Hot: Firing up the Tumor Microenvironment. *Trends Cancer* 2020;6:605–18.
23 Sautès-Fridman C, Petitprez F, Calderaro J, *et al*. Tertiary lymphoid structures in the era of cancer immunotherapy. *Nat Rev Cancer* 2019;19:307–25.
24 Schumacher TN, Thommen DS. Tertiary lymphoid structures in cancer. *Science* 2022;375:eabf9419.
25 Li S, Mwakalundwa G, Skinner PJ. In Situ MHC-tetramer Staining and Quantitative Analysis to Determine the Location, Abundance, and Phenotype of Antigen-specific CD8 T Cells in Tissues. *J Vis Exp* 2017.:56130.
26 Abdelaal HM, Cartwright EK, Skinner PJ. Detection of Antigen-Specific T Cells Using In Situ MHC Tetramer Staining. *Int J Mol Sci* 2019;20:5165.
27 Workel HH, Lubbers JM, Arnold R, *et al*. A Transcriptionally Distinct CXCL13+CD103+CD8+ T-cell Population Is Associated with B-cell Recruitment and Neoantigen Load in Human Cancer. *Cancer Immunol Res* 2019;7:784–96.
28 Li H, Ding J-Y, Zhang M-J, *et al*. Tertiary lymphoid structures and cytokines interconnections: The implication in cancer immunotherapy. *Cancer Lett* 2023;568:216293.
29 Cabrita R, Lauss M, Sanna A, *et al*. Tertiary lymphoid structures improve immunotherapy and survival in melanoma. *Nature New Biol* 2020;577:561–5.
30 Helmink BA, Reddy SM, Gao J, *et al*. B cells and tertiary lymphoid structures promote immunotherapy response. *Nature New Biol* 2020;577:549–55.
31 Richards DM, Hettinger J, Feuerer M. Monocytes and macrophages in cancer: development and functions. *Cancer Microenviron* 2013;6:179–91.
32 DeNardo DG, Ruffell B. Macrophages as regulators of tumour immunity and immunotherapy. *Nat Rev Immunol* 2019;19:369–82.
33 Murray PJ, Allen JE, Biswas SK, *et al*. Macrophage activation and polarization: nomenclature and experimental guidelines. *Immunity* 2014;41:14–20.
34 Burtness B, Rischin D, Greil R, *et al*. Pembrolizumab Alone or With Chemotherapy for Recurrent/Metastatic Head and Neck Squamous Cell Carcinoma in KEYNOTE-048: Subgroup Analysis by Programmed Death Ligand-1 Combined Positive Score. *JCO* 2022;40:2321–32.
35 Cohen EEW, Bell RB, Bifulco CB, *et al*. The Society for Immunotherapy of Cancer consensus statement on immunotherapy for the treatment of squamous cell carcinoma of the head and neck (HNSCC). *j immunotherapy cancer* 2019;7:184.
36 Haring CT, Kana LA, Dermody SM, *et al*. Patterns of recurrence in head and neck squamous cell carcinoma to inform personalized surveillance protocols. *Cancer* 2023;129:2817–27.
37 Barbosa MMP, Lopez AJ, Uyehara R, *et al*. Abstract 6347: Preliminary results of an exploratory phase I clinical trial of anchored canine interleukin-12 (cANK-101) in dogs with advanced oral malignant melanoma. *Cancer Res* 2023;83:6347.
38 Jorgovanovic D, Song M, Wang L, *et al*. Roles of IFN-γ in tumor progression and regression: a review. *Biomark Res* 2020;8:49.
39 Fabian KP, Wolfson B, Hodge JW. From Immunogenic Cell Death to Immunogenic Modulation: Select Chemotherapy Regimens Induce a Spectrum of Immune-Enhancing Activities in the Tumor Microenvironment. *Front Oncol* 2021;11:728018.
40 Fabian KP, Kowalczyk JT, Reynolds ST, *et al*. Dying of Stress: Chemotherapy, Radiotherapy, and Small-Molecule Inhibitors in Immunogenic Cell Death and Immunogenic Modulation. *Cells* 2022;11:3826.
41 Curry JM, Sprandio J, Cognetti D, *et al*. Tumor microenvironment in head and neck squamous cell carcinoma. *Semin Oncol* 2014;41:217–34.
42 Kumar AT, Knops A, Swendseid B, *et al*. Prognostic Significance of Tumor-Associated Macrophage Content in Head and Neck Squamous Cell Carcinoma: A Meta-Analysis. *Front Oncol* 2019;9:656.
43 Gschwandtner M, Derler R, Midwood KS. More Than Just Attractive: How CCL2 Influences Myeloid Cell Behavior Beyond Chemotaxis. *Front Immunol* 2019;10:2759.
44 Chen S, Saeed AFUH, Liu Q, *et al*. Macrophages in immunoregulation and therapeutics. *Signal Transduct Target Ther* 2023;8:207.
45 Mosser DM, Hamidzadeh K, Goncalves R. Macrophages and the maintenance of homeostasis. *Cell Mol Immunol* 2021;18:579–87.
46 House IG, Savas P, Lai J, *et al*. Macrophage-Derived CXCL9 and CXCL10 Are Required for Antitumor Immune Responses Following Immune Checkpoint Blockade. *Clin Cancer Res* 2020;26:487–504.
47 Sagiv-Barfi I, Czerwinski DK, Shree T, *et al*. Intratumoral immunotherapy relies on B and T cell collaboration. *Sci Immunol* 2022;7:eabn5859.
48 Messina JL, Fenstermacher DA, Eschrich S, *et al*. 12-Chemokine gene signature identifies lymph node-like structures in melanoma: potential for patient selection for immunotherapy. *Sci Rep* 2012;2:765.
49 Hiraoka N, Ino Y, Yamazaki-Itoh R, *et al*. Intratumoral tertiary lymphoid organ is a favourable prognosticator in patients with pancreatic cancer. *Br J Cancer* 2015;112:1782–90.
50 Coppola D, Nebozhyn M, Khalil F, *et al*. Unique Ectopic Lymph Node-Like Structures Present in Human Primary Colorectal Carcinoma Are Identified by Immune Gene Array Profiling. *Am J Pathol* 2011;179:37–45.
51 Wood O, Woo J, Seumois G, *et al*. Gene expression analysis of TIL rich HPV-driven head and neck tumors reveals a distinct B-cell signature when compared to HPV independent tumors. *Oncotarget* 2016;7:56781–97.
52 Ruffin AT, Cillo AR, Tabib T, *et al*. B cell signatures and tertiary lymphoid structures contribute to outcome in head and neck squamous cell carcinoma. *Nat Commun* 2021;12:3349.
53 Vaccaro A, van de Walle T, Ramachandran M, *et al*. Of mice and lymphoid aggregates: modeling tertiary lymphoid structures in cancer. *Front Immunol* 2023;14:1275378.
54 Wirsing AM, Ervik IK, Seppola M, *et al*. Presence of high-endothelial venules correlates with a favorable immune microenvironment in oral squamous cell carcinoma. *Mod Pathol* 2018;31:910–22.
55 van Herpen CML, van der Laak JAWM, de Vries IJM, *et al*. Intratumoral recombinant human interleukin-12 administration in head and neck squamous cell carcinoma patients modifies locoregional lymph node architecture and induces natural killer cell infiltration in the primary tumor. *Clin Cancer Res* 2005;11:1899–909.
56 Nashi E, Wang Y, Diamond B. The role of B cells in lupus pathogenesis. *Int J Biochem Cell Biol* 2010;42:543–50.

J Immunother Cancer: first published as 10.1136/jitc-2024-009712 on 23 October 2024. Downloaded from http://jitc.bmj.com/ on October 24, 2024 at NIH Library Consortia. Protected by copyright.